Modulation of Electronic Properties of π-Conjugated Copolymers Derived from Naphtho[1,2-b:5,6-b′]dithiophene Donor Unit: A Structure–Property Relationship Study

Pranabesh Dutta,[1] Hanok Park,[1] Minjae Oh,[1] Sushil Bagde,[1] In Nam Kang,[2] Soo-Hyoung Lee[1]

[1]School of Semiconductor and Chemical Engineering, Chonbuk National University, Duckjin-dong 664-14, Jeonju 561–756, Republic of Korea

[2]Department of Chemistry, The Catholic University, 43-1, Yeokaok2-dong, Wonmi-gu, Buchen-si, Gyeonggi-do 420–743, Republic of Korea

Correspondence to: S.-H. Lee (E-mail: shlee@shlee66@jbnu.ac.kr)

ABSTRACT: A set of three donor-acceptor conjugated (D-A) copolymers were designed and synthesized via Stille cross-coupling reactions with the aim of modulating the optical and electronic properties of a newly emerged naphtho[1,2-b:5,6-b′]dithiophene donor unit for polymer solar cell (PSCs) applications. The **PTNDTT-BT**, **PTNDTT-BTz**, and **PTNDTT-DPP** polymers incorporated naphtho[1,2-b:5,6-b′]dithiophene (**NDT**) as the donor and 2,2′-bithiazole (**BTz**), benzo[1,2,5]thiadiazole (**BT**), and pyrrolo[3,4-c]pyrrole-1,4(2H,5H)-dione (**DPP**), as the acceptor units. A number of experimental techniques such as differential scanning calorimetry, thermogravimetry, UV–vis absorption spectroscopy, cyclic voltammetry, X-ray diffraction, and atomic force microscopy were used to determine the thermal, optical, electrochemical, and morphological properties of the copolymers. By introducing acceptors of varying electron withdrawing strengths, the optical band gaps of these copolymers were effectively tuned between 1.58 and 1.9 eV and their HOMO and LUMO energy levels were varied between −5.14 to −5.26 eV and −3.13 to −3.5 eV, respectively. The spin-coated polymer thin film exhibited p-channel field-effect transistor properties with hole mobilities of 2.73×10^{-3} to 7.9×10^{-5} cm^2 V^{-1} s^{-1}. Initial bulk-heterojunction PSCs fabricated using the copolymers as electron donor materials and [6,6]-phenyl C71 butyric acid methyl ester (PC$_{71}$BM) as the acceptor resulted in power conversion efficiencies in the range of 0.67–1.67%. © 2013 Wiley Periodicals, Inc. J. Polym. Sci., Part A: Polym. Chem. **2013**, 51, 2948–2958

KEYWORDS: bulk-heterojunction; conjugated polymers; electrochemistry; organic field-effect transistors; polymer solar cells; structure-property relations

INTRODUCTION The emergence of cost-effective renewable energy source alternatives to existing silicon photovoltaics has enormously increased the worldwide academic and industrial interest in so-called bulk-heterojunction (BHJ) polymer solar cells (PSCs) because they hold the potential to be fabricated on flexible modules and large-area substrates via solution-casting at a much lower cost.[1–8] In BHJ PSCs, conjugated copolymers with an alternating donor-acceptor (D-A) structure have so far shown a great promise, yielding power conversion efficiency (PCE) values >8%.[9–15] Development of new, low band gap conjugated polymers based on novel donor or acceptor units have greatly advanced the progress of PSCs. The increased light harvesting ability and tunable electronic and optoelectronic properties of D-A conjugated copolymers have made them particularly attractive as one of the key elements in the active layers for PSCs, especially for the optimization of device parameters including short-circuit current and open circuit voltage. After years of extensive optimization in molecular structures, currently, a great number of D-A conjugated systems are capable of delivering high PCEs, thus generating an exciting library of copolymers in PSCs.[16–24]

Towards the development of new efficient D-A conjugated polymers for PSC applications, π-conjugated rigidly fused thiophene-based molecular semiconductors have so far been particularly attractive due to their rigid, coplanar conformation, which facilitates effective packing of the conjugated backbone and improves the charge transport mobility. A number of π-conjugated rigidly fused donor units including fluorine,[25] silafluorene,[26] carbazole,[27] benzo[1,2-b:4,5-b′]-dithiophene,[17,18,22,24,28] cyclopenta[2,1-b:3,4-b′]dithiophene,[29] dithieno[3,2-b:2′,3′-d]-silole,[20,30] and indacenodithiophene,[31] as well as acceptors such as 2,1,3-benzothiadiazole,[32] bithiazole,[33] thiazolothiazole,[34] quinoxaline,[35] thieno[3,4-c]pyrrole-
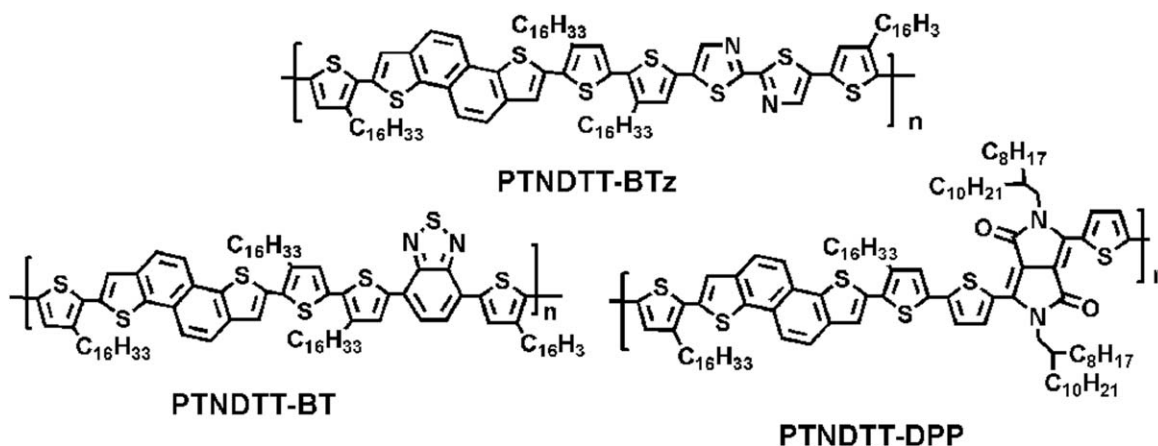
CHART 1 Chemical structures of the polymers reported in this work.

4,6-dione,[36] pyrrolo[3,4-c]-pyrrole-1,4-dione,[37] etc. have been incorporated in D-A conjugated polymer backbones and explored for their potential in PSCs. Owing to the high oxidative stability and excellent charge transport mobility, naphthodithiophene derivatives consisting of a naphthalene unit with thiophene units condensed to it have also recently attracted considerable attention as potential π-conjugated fused thiophene building blocks in conjugated polymers.[38–40] You and coworkers have conducted extensive investigations of the photovoltaic performance of naphtho[2,1-b:3,4-b′]dithiophene containing D-A conjugated polymers for PSC applications.[41] A structural analog to naphtho[2,1-b:3,4-b′]dithiophene, naphtho[1,2-b:5,6-b′]dithiophene, with two thiophene rings fused at the end of a naphthalene unit has also emerged recently as a promising p-type organic semiconductor in field-effect transistor (OFET) devices.[42] Polymers containing this naphtho[1,2-b:5,6-b′]dithiophene unit have shown high thermal stability, relatively low-lying HOMO levels and impressive hole mobilities of 0.5 cm^2 V^{-1} s^{-1} with on/off current ratios (I_{on}/I_{off}) of up to 10^8 in OFET devices.[43] However, the synthesis and use of this unit in photovoltaic application has not been reported since the first reports by Osaka and coworkers concerning OFET devices. By attaching alkylated thiophenes to the 2,7-position of naphtho[1,2-b:5,6-b′]dithiophene core, recently, we have shown for the first time that this naphthodithiophene analog can also be used as a novel building block to construct π-conjugated small molecules for organic solar cell applications.[44] To expand its scope in PSC applications, we concurrently studied the use of the naphtho[1,2-b:5,6-b′]dithiophene heterocycle as the donor unit in D-A conjugated polymer. The first synthesis and photovoltaic application of thiophene-bridged naphtho[1,2-b:5,6-b′]dithiophene-containing D-A conjugated copolymer in combination with a quinoxaline acceptor moiety resulted in a low band gap (1.77 eV) polymer with promising photovoltaic device properties and a PCE of 1.44%.[45] More recently, Osaka et al. has reported the synthesis and characterization of two new naphtho[1,2-b:5,6-b′]dithiophene-based D–A copolymers in combination with benzothiadiazole and naphthobisthiadiazole acceptor units for OFET and OPV device applications.[46] The copolymer based on naphtho[1,2-b:5,6-b′]dithiophene-

naphthobisthiadiazole, with longer decyltetradecyl side chains afforded excellent semiconducting behavior with field-effect mobility of ∼0.5 cm^2 V^{-1} s^{-1} and the PCE of ∼5%, that demonstrate the potential of the naphtho[1,2-b:5,6-b′]dithiophene fused unit in optoelectronic applications.

To investigate further the effect of acceptor groups on the electronic and optoelectronic properties of naphtho[1,2-b:5,6-b′]dithiophene-based polymers and thus, learn more about the structure-property relationship, we designed and synthesized a set of three D-A conjugated copolymers, poly[2,7-bis(3-hexadecylthiophene-2-yl) naphtho [1,2-b:5,6-b′] dithiophene-5,5′-diyl-alt−5,5-bis(4-hexadecylthiophene-2-yl)−2,2′-bithiazole-5,5′-diyl] (**PTNDTT-BTz**), poly[2,7-bis(3-hexadecyl thiophene-2-yl)naphtho[1,2-b:5,6-b′]dithiophene-5,5′-diyl-alt−4,7-bis(4-hexadecylthiophen-2-yl)benzo[1,2,5]thiadiazole-5,5′-diyl] (**PTNDTT-BT**), and poly[2,7-bis(3-hexadecylthiophene-2-yl)naphtho[1,2-b:5,6-b′]dithiophene-5,5′-diyl-alt−3,6-bis(5-thiophene-2-yl)−2,5-bis(2-octyl-1dodecyl)pyrrolo[3,4-c]pyrrolo-1,4(2H,5H)-dione-5,5′-diyl] (**PTNDTT-DPP**), that use naphtho[1,2-b:5,6-b′]dithiophene as the donor unit and 2,2′-bithiazole (**BTz**), benzo[1,2,5]thiadiazole (**BT**), and pyrrolo[3,4-c]pyrrole-1,4(2H,5H)-dione (**DPP**) as acceptor units (Chart 1). The influence of the different acceptor groups on the field-effect transistor behaviors, and the optoelectronics and photovoltaic properties was examined.

RESULTS AND DISCUSSION

Synthesis and Thermal Stability

The general synthetic routes for the monomers and copolymers are presented in Schemes 1 and 2, respectively. Monomer 2,7-bis(3-hexadecylthiophene-2-yl)naphtho[1,2-b:5,6-b′]dithiophene (**8**) was synthesized starting from NDT (**5**) in three steps in high yield.[44] A Pd(PPh$_3$)$_4$-catalyzed Suzuki coupling reaction between 5,5′-dibromo-2,2′-bithiazole (**10**) and 2-(4-hexadecylthiophen-2-yl)−4,4′,5,5′-tetramethyl-1,3,2-dioxaborolane resulted in 5,5′-bis(4-hexadecylthiophen-2-yl)−2,2′-bithiazole (**11**), which was subsequently brominated with NBS to afford the monomer 5,5′-bis(5-bromo-4-hexadecylthiophen-2-yl)−2,2′-bithiazole (**12**). A similar strategy was adapted to generate the 4,7-bis(5-bromo-4-
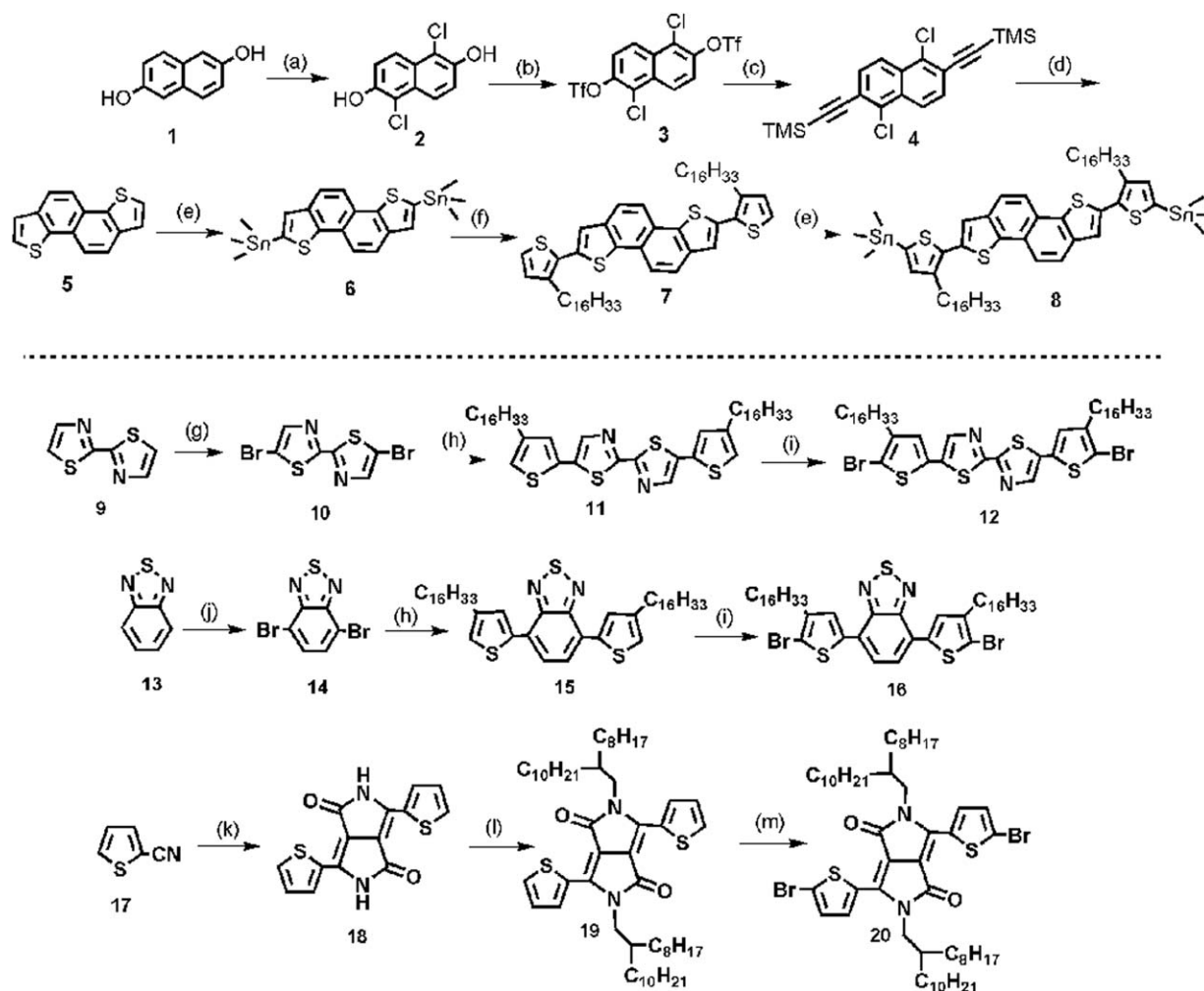
SCHEME 1 Synthetic scheme for Monomers. Conditions: (a) SO2Cl2, AcOH, 0–5 °C, 5 h; (b) Trifluoromethanesulfonic anhydride (Tf2O), pyridine, 0–5 °C, 18 h; (c) ethynyltrimethylsilane, CuI, Pd(PPh)2Cl2, NEt3, reflux, 20 h; (d) Na2S.9H2O, N-methyl-2-pyrrolidone (NMP), 185 °C, 12 h; (e) butyllithium, −78 °C, 30 min, trimethyltin chloride, 2 h; (f) 2-bromo-3-hexadecylthiophene, Pd(PPh3)2Cl2, 120 °C, 24 h; (g) NBS, DMF, 60 °C; (h) 2-(4-hexadecylthiophen-2-yl)−4,4′,5,5′-tetramethyl-1,3,2-dioxaborolane, Pd(PPh3)4, 2 M K2CO3, toluene, reflux; (i) NBS, CHCl3/AcOH, 1 h; (j) Br2, HBr, reflux, 6 h; (k) dimethyl succinate, t-BuOK, t-amyl alcohol, 110 °C, 4 h; (l) 2-octyl-1-dodecyl bromide, DMF, K2CO3, 140 °C, 12 h; (m) NBS, DMF, 15 h.

hexadecylthiophen-2-yl)benzo[c][1,2,5]thiadiazole (**16**) monomer. The monomer 3,6-bis(5-bromothiophen-2-yl) −2,5-bis (2-octyl-1dodecyl)pyrrolo[3,4-c]pyrrole-1,4(2H,5H)-dione (**20**) was prepared following a similar method, previously reported by our group.[45(b)] The copolymers were synthesized via a Stille cross-coupling polymerization in the presence of Pd2(dba)3 and tri(o-tolyl)phosphine [P(o-tolyl)] as catalyst and ligand, respectively. The detailed synthetic procedures for both monomers and polymers are described in the Supporting Information. The chemical structures of the copolymers **PTNDTT-BTz**, **PTNDTT-BT**, and **PTNDTT-DPP** were confirmed by ^{1}H NMR spectroscopy. The spectra have been included in Supporting Information. All three polymers showed good solubility in common organic solvents such as chloroform, chlorobenzene, and tetrahydrofuran. The molecular weight (M_w) and polydispersity index (PDI, M_w/M_n) of each of the resulting copolymers was

determined by a gel permeation chromatography (GPC) using polystyrenes as standards and chloroform as eluent. The molecular weight and PDI of the resulting copolymers are listed in Table 1. The **PTNDTT-BTz** and **PTNDTT-BT** had number average molecular weights (M_n) of 6.41 and 8.91 kg mol^{-1}, respectively, and PDIs of 1.07 and 1.06, respectively. The molecular weight of **PTNDTT-DPP** was relatively higher with M_n and PDI values of 191.79 kg mol^{-1} and 5.1, respectively. The broad PDI of **PTNDTT-DPP** suggests strong intermolecular interactions and polymer aggregation presumably a result of the presence of branched alkyl chain in the DPP unit.[46,47]

Thermogravimetric analysis (TGA) and differential scanning calorimetry (DSC) were performed to investigate the thermal stability and the thermal transitions of the copolymers. The TGA analysis (Fig. S6, Supporting Information) revealed that
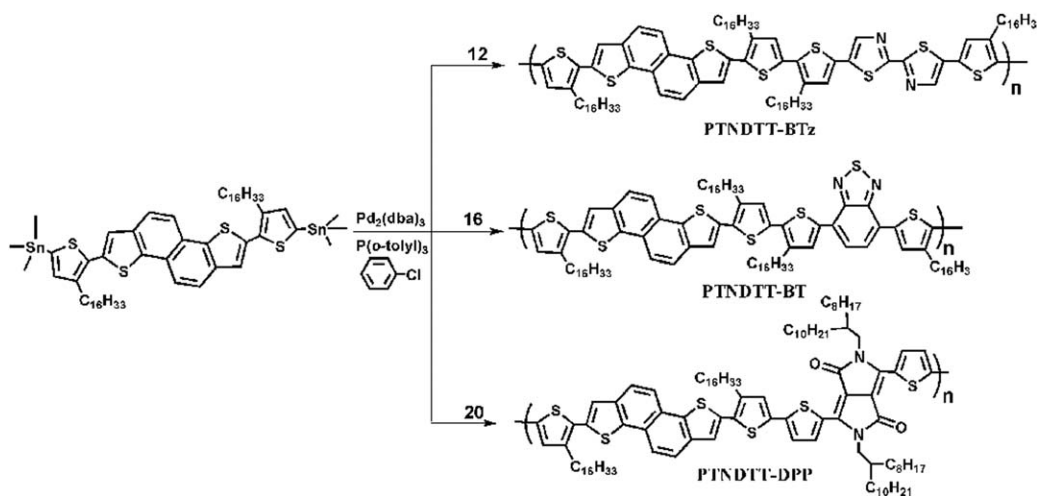
SCHEME 2 Synthetic scheme for polymers.

all three copolymers had high decomposition temperatures (near or over 300 °C), indicating excellent thermal stability, a prerequisite for photovoltaic applications. The high thermal stability of the copolymers prevents degradation or deformation under thermal annealing conditions used in the fabrication of photovoltaic devices. When investigating the thermal transitions with DSC (Supporting Information Fig. S7), none of the samples could exhibit distinct thermal transition temperatures in the 40–280 °C temperature range scanned.

Optical Properties

The absorption spectra of the copolymers both in dichlorobenzene solutions and on solid thin films are shown in Figure 1. The relevant optical properties including absorption peak (λ_{max}), absorption onset (λ_{onset}), and optical band gap (E_g^{opt}) for the **PTNDTT-BTz**, **PTNDTT-BT**, and **PTNDTT-DPP** polymers are compiled in Table 2. In solution, as shown in Figure 1(a), the copolymer **PTNDTT-BTz** featuring a bithiazole moiety as an acceptor has a narrow (350–650 nm) absorption band, the maxima of which is located at 466 nm. In marked contrast, the absorption spectra for the **PTNDTT-BT** and **PTNDTT-DPP** polymers including benzothiadiazole and diketopyrrolopyrrole acceptors, respectively, are broad and characterized by two prominent absorption bands in the range of ∼340–470 nm and ∼470–740 nm for

PTNDTT-BT and ∼340–520 nm and ∼520–880 nm for **PTNDTT-DPP**. These absorption bands can be assigned to the π-π^* transition of the donor/acceptor (NDT/BT or NDT/DPP) conjugated backbone and the corresponding intramolecular charge transfer transition, respectively. The absorption maxima (λ_{max}) for **PTNDTT-BT** are located at 417 and 546 nm, while those for **PTNDTT-DPP** are at 415 and 659 nm. Notably, the longer wavelength absorption band is more intense and broad for **PTNDTT-DPP** the maximum of which is significantly red-shifted by ∼113 nm relative to **PTNDTT-BT**, a clear indication of the stronger electron-withdrawing capability of DPP and its strengthening of the D/A interactions in **PTNDTT-DPP** as compared to those of BT in **PTNDTT-BT**. Figure 1(b) presents the thin film absorption spectra of the copolymers. As can be seen from the figure, the copolymers' thin film absorption maxima are red-shifted relative to those of the solutions, an indication of π-π interchain association and aggregation. The largest solution-to-film red shift was observed for the lowest energy absorption peaks of **PTNDTT-BT** (∼86 nm), which is much larger shift than that of **PTNDTT-BTz** (∼36 nm). More interestingly, the thin-film absorption spectra of **PTNDTT-DPP** exhibited well-defined vibronic splitting peaks at 663 and 738 nm, similar to what is seen in regioregular semiconducting polymers such as HT-P3HT,[48] and is indicative of the efficient π-stacking and enhanced intermolecular interactions for **PTNDTT-DPP** films.[49] The thin film optical bandgaps (E_g) were 1.73, and 1.51 eV for **PTNDTT-BT** and **PTNDTT-DPP**, respectively; significantly lower than that of **PTNDTT-BTz** (1.98 eV).

Electrochemical Properties

To examine the oxidation and reduction potentials and estimate the copolymers' highest occupied molecular orbital (HOMO) and lowest occupied molecular oribital (LUMO) energy levels cyclic voltammetry (CV) was performed using Ag/AgCl as the reference electrode in a 0.1 M solution of Bu_4NPF_6 in acetonitrile at room temperature under argon at a scan rate of 50 mV s^{-1}. During calibration, the half-wave

TABLE 1 Molecular Weight and Thermal Properties of Copolymers

Polymers	[a]M_n (kg mol^{-1})	[a]M_w (kg mol^{-1})	[a]PDI	[b]T_d (°C)
PTNDTT-BTz	6.41	6.9	1.07	303
PTNDTT-BT	8.91	9.51	1.06	297
PTNDTT-DPP	191.79	979.73	5.1	370

[a] M_n, M_w, and PDI of the polymers were determined by GPC using polystyrene standards in chloroform.
[b] Temperature at 5% weight loss with a heating rate of 10 °C min^{-1} under nitrogen.
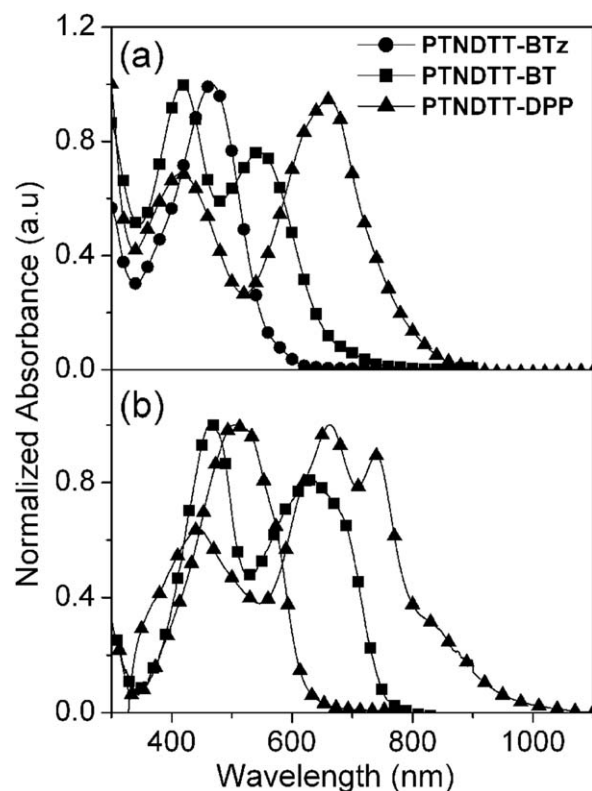
FIGURE 1 Normalized UV–vis absorption spectra of copolymers in dilute *o*-DCB solution (a) and thin film (b) at room temperature.

potential of the ferrocene/ferrocenium (Fc/Fc$^+$) redox couple, which has an absolute energy level of −4.8 eV relative to the vaccum level was located at 0.4 V. Thus, the HOMO and LUMO energy levels of the copolymers were calculated using the equations $E_{HOMO} = -(E^{ox}_{onset} + 4.40;$ eV) and $E_{LUMO} = -(E^{Red}_{onset} + 4.40;$ eV), respectively. The CV curves for the polymers are shown in Figure 2. As displayed, the copolymers **PTNDTT-BTz**, and **PTNDTT-BT**, undergo completely irreversible oxidation and reduction peaks, while a partially reversible oxidation peak and an irreversible reduction peak were observed for **PTNDTT-DPP**. The onset oxidation and reduction potentials are listed with the calculated

HOMO and LUMO energy levels of the copolymers in Table 2. The HOMO values for **PTNDTT-BTz, PTNDTT-BT,** and **PTNDTT-DPP** were estimated as −5.26, −5.14, and −5.22 eV, while the calculated LUMO energy levels were −3.26, −3.13, and −3.5 eV, respectively. The small variation in HOMO values (∼−5.14 to −5.26 eV) for the copolymers can be attributed to the presence of an identical donor unit (thiophene-bridged naphthodithiophene), since the HOMO for a D-A conjugated polymer is more localized on the donor. As a result of different acceptors content, the LUMO levels of the copolymers varied more, from −3.13 to −3.5 eV. The fact that **PTNDTT-DPP** has much lower LUMO value (−3.5 eV) than **PTNDTT-BTz** (−3.26 eV) and **PTNDTT-BT** (−3.13 eV) could be explained by the much stronger electron-withdrawing ability of the DPP acceptor unit with respect to the BT and BTz moieties. The electrochemical band gaps ($E_{g, ec}$) of the three polymers range from 1.7 to 2.0 eV. Although the $E_{g, ec}$ of **PTNDTT-BTz** (2 eV), estimated from the difference between the HOMO and LUMO energy levels, was consistent with its optical band gap (1.98 eV), the $E_{g, ec}$ values for **PTNDTT-BT** (2.01 eV) and **PTNDTT-DPP** (1.72 eV) were slightly larger (0.2 − 0.3 eV) than their corresponding optical band gaps. This difference between the electrochemical and optical band gaps for **PTNDTT-BT** and **PTNDTT-DPP** could presumably be a result of the exciton binding energies of the polymers or possibly an interfacial charge injection barrier during CV measurement.[50] When considering the implementation of any polymers in photovoltaic device applications, the positions of the HOMO and LUMO levels are important parameters that should be matched carefully with that of the PCBM acceptor to facilitate exciton dissociation. As evident from the band diagram (Fig. 3), the cenergy levels of all the copolymers have LUMO levels above −3.6 eV, therefore maintaining the required offsets (0.3 eV) between the copolymer LUMO levels and PC$_{71}$BM (−3.9 eV), which ensures sufficient driving force for charge transfer in photovoltaic devices with the acceptor PC$_{71}$BM.

Field-Effect Transistor Characteristics

The field-effect carrier mobilities of the polymers were evaluated by fabricating thin-film transistors (TFTs) devices with a bottom-gate top-contact configuration (channel length = 12 μm, width = 120 μm) on an n-doped silicon wafer with evaporated gold source and drain electrodes and an

TABLE 2 Optical, Electrochemical, and Field-Effect Transistors (FET) Properties of the Copolymers

Polymer	$^a\lambda_{max}$ (nm)	$^b\lambda_{max}$ (nm)	$^b\lambda_{onset}$ (nm)	$^cE_g^{opt}$ (eV)	$^dE_{ox}$ (V)/^{e} HOMO (eV)	$^dE_{Red}$ (V)/^{e} LUMO (eV)	$^f\mu$ (cm^2 V^{-1} s^{-1})	$^fI_{on}/I_{off}$
PTNDTT-BTz	466	502	624	1.98	0.86/−5.26	−1.17/−3.26	7.9 × 10^{-5}	2 × 10^2
PTNDTT-BT	417, 546	466, 632	752	1.73	0.74/−5.14	−1.27/−3.13	2.73 × 10^{-3}	10^2
PTNDTT-DPP	415, 659	444, 663	819	1.51	0.82/−5.22	−0.9/−3.5	2.8 × 10^{-4}	10^2

^{a} Measured in chloroform solution.
^{b} Spin-coated film from chloroform solution.
^{c} Optical band gap, $E_{g, opt} = 1240/(\lambda_{onset})_{film}$.
^{d} Potential determined by cyclic voltammetry in 0.10 M Bu$_4$NPF$_6$—CH$_3$CN.

^{e} HOMO = −(4.4 + $E_{ox, onset}$) (eV); LUMO = −(4.4 + $E_{red, onset}$).
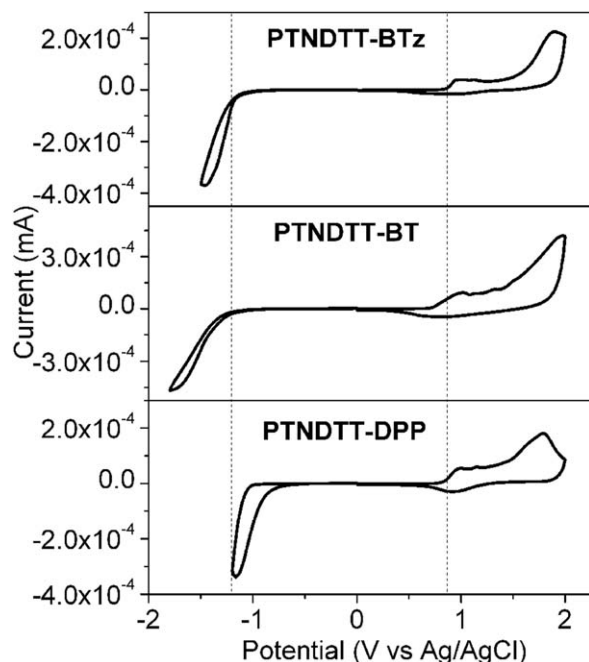^{f} Hole mobilities (μ) and on-off ratios (I_{on}/I_{off}) were extracted from transfer curves in the saturation regime.

FIGURE 2 Cyclic voltammogram of copolymer films deposited on ITO glass in an acetonitrile solution of 0.1 M n-Bu$_4$NF$_6$ at a scan rate of 50 mV s^{-1}.

octyltrichlorosilane (OTS-8)-modified (300 nm) silicon dioxide (SiO$_2$) gate dielectric. The gold (Au) source/drain electrode pairs (70 nm) were deposited on top of the thin films by high vacuum thermal evaporation through a shadow mask to define the channel length. The polymers were dissolved to a concentration of 0.5 wt % in o-dichlorobenzene and were spin-coated at 1500 rpm for 50 s to a thickness of 50 nm, followed by an annealing process. All device fabrication procedures and measurements were carried out at room temperature under ambient conditions. Hole mobility (μ_h) was extracted from the slope of the square root of the plot of the drain current versus V_G from the following equation:

$$I_{DS} = \frac{W}{2L} C_i \mu (V_G - V_T)^2 \qquad (1)$$

where I_{DS} is the drain-source current in the saturated region, W and L are the channel width and length, respectively, μ is the field-effect mobility, C_i is the capacitance per unit area of the insulation layer (SiO$_2$, 300 nm), and V_G and V_T are the gate and threshold voltages, respectively. Figure 4 shows the transfer curves with respect to V_G. The copolymers exhibited p-channel FET responses. The mobilities and on/off ratios of TFTs fabricated using the copolymers are included in Table 2. All three copolymers exhibited typical p-type organic semiconductor characteristics and their hole mobilities were estimated to be 7.9×10^{-5}, 2.73×10^{-3}, and 2.8×10^{-4} cm^2 V^{-1} s^{-1} for **PTNDTT-BTz**, **PTNDTT-BT,** and **PTNDTT-DPP**, respectively. The hole mobilities for **PTNDTT-BT** and **PTNDTT-DPP** were within the desired range for efficient PSC applications, that is, near or above 10^{-3} cm^2 V^{-1} s^{-1},

allowing for an efficient charge extraction and a good fill factor (FF). Surprisingly, the mobility of **PTNDTT-BTz** copolymer was significantly lower than the others, which could be ascribed to its lower molecular weight.[51] To gain insight into the factors that differentiate the transistors properties of the copolymers, the solid state molecular packing of **PTNDTT-BTz**, **PTNDTT-BT,** and **PTNDTT-DPP** films (~120 nm) were investigated with X-ray diffraction (XRD) studies. Figure 4(d) shows the XRD patterns for the copolymers. **PTNDTT-BTz** film showed a very weak (100) diffraction peak centered at $2\theta = 3.7°$ (d-spacing of 23.78 Å), suggesting that this polymer is largely amorphous in nature. A similar pattern ($2\theta = 3.67°$, d-spacing = 24.04 Å) was observed for the **PTNDTT-DPP** film, though its intensities were stronger.

In marked contrast, in addition to the strong and intense peak located at $2\theta = 3.64°$ (d-spacing of 24.24 Å), corresponding to the regular lamellar stacking, the **PTNDTT-BT** film exhibited up to the second and third order diffraction peaks at 4.92° (d-spacing = 17.93 Å), 7.35° (d-spacing = 12.01 Å), and 12.2° (d-spacing = 7.24 Å), indicating that **PTNDTT-BT** achieves a high degree of crystallinity.[52] The greater lamellar crystallinity of the **PTNDTT-BT** film as observed in XRD appears to explain its one or two order greater carrier mobility as compared to **PTNDTT-BTz** and **PTNDTT-DPP** copolymers. Although, **PTNDTT-BTz** exhibits a stronger crystalline peak in its XRD pattern, we did not observe any XRD feature related to π-π stacking, indicating that this copolymer adopts a layered structure with an edge-on orientation related to the substrate.[53] Some possible mode of organization of alkyl chains for **PTNDTT-BT** that led to its higher order structure is further presented in Supporting Information Figure S8.

Photovoltaic Properties

To examine the potential of the copolymers in photovoltaic applications, BHJ PSC devices were fabricated with the layered ITO/PEDOT:PSS/polymer:PC$_{71}$BM/LiF/Al configuration. The copolymers were blended with PC$_{71}$BM in various polymer:PC$_{71}$BM ratios (1:1 to 1:4) and spin coated from o-dichlorobenzene solutions on top of the PEDOT:PSS layer (20 nm). We preferred to use PC$_{71}$BM over PC$_{61}$BM, as the former acceptor has a stronger visible absorption profile
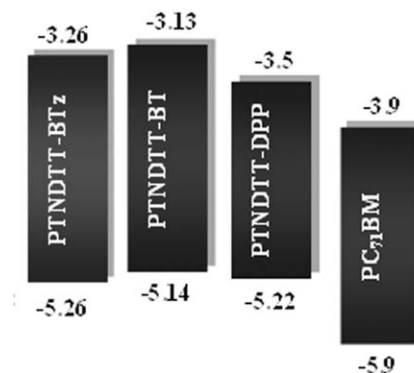

FIGURE 3 HOMO and LUMO energy diagram for the polymers (**PTNDTT-BTz**, **PTNDTT-BT**, and **PTNDTT-DPP**) and PC$_{71}$BM.
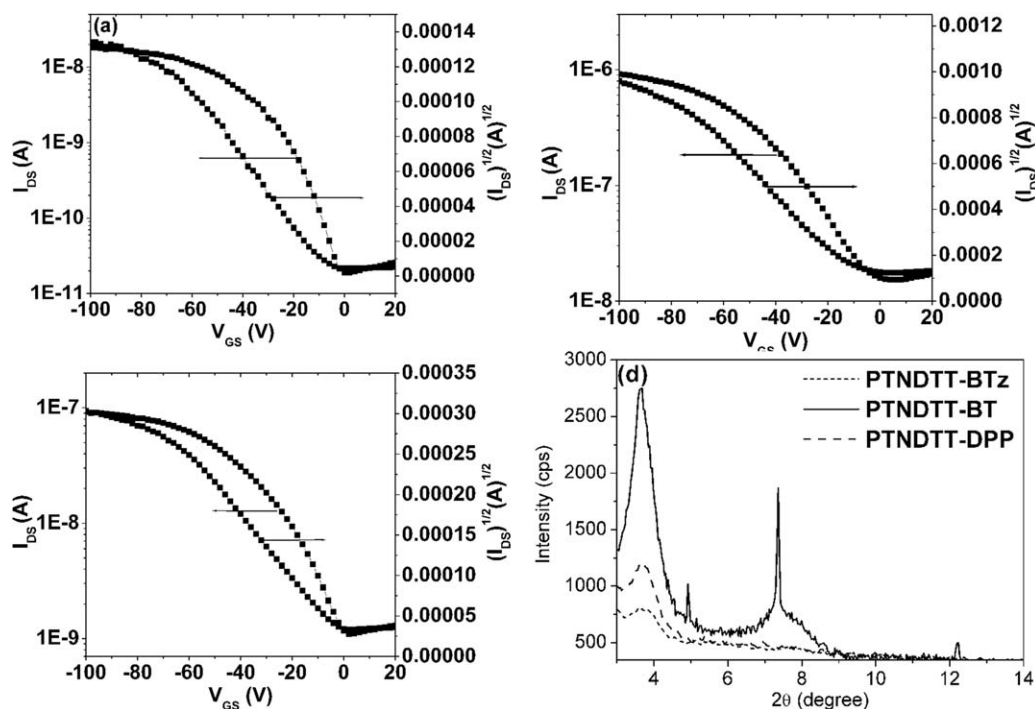
FIGURE 4 Transfer characteristics of (a) **PTNDTT-BTz-**, (b) **PTNDTT-BT-**, and (c) **PTNDTT-DPP**-based bottom-gate top-contact thin film transistors (TFT) devices; (d) XRD scattering patterns of the copolymers.

than the later one. Active layer thicknesses were optimized at 70–80 nm for **PTNDTT-BTz** and **PTNDTT-BT** and at 90–100 nm for **PTNDTT-DPP**. The devices were characterized both in the dark and under a solar simulator (AM 1.5 illuminations, 100 mW cm^{-2}). The current-voltage characteristics (*J-V*) of some representative PSCs based on **PTNDTT-BTz**, **PTNDTT-BT,** and **PTNDTT-DPP** are presented in Figure 5(a) and the detailed device parameters for all the cells have been included in Table 3. As shown in Table 3, the short circuit current (J_{sc}), open circuit voltage (V_{oc}), FF, and PCE of the PSC based on **PTNDTT-BTz**:PC$_{71}$BM (1:4) reached 3.15 mA cm^{-2}, 0.70 V, 0.34, and 0.76% respectively, while the

device based on **PTNDTT-DPP**:PC$_{71}$BM blend at 1:1 ratio displayed a maximum PCE of 1.42%, with a J_{sc} of 4.37 mA cm^{-2}, V_{oc} of 0.62 V, and FF of 0.53. The best photovoltaic performance was seen in the **PTNDTT-BT**:PC$_{71}$BM (1:1)-based devices with a J_{sc} of 4.67 mA cm^{-2}, a V_{oc} of 0.63 V, a FF of 0.54, and a PCE of 1.62%. The devices fabricated using the **PTNDTT-BT** and **PTNDTT-DPP** copolymers offer higher short circuit currents than those made with the **PTNDTT-BTz** copolymer, a fact that could be explained by the greater light absorption of **PTNDTT-BT** and **PTNDTT-DPP** as compared with **PTNDTT-BTz**. Moreover, the ability to attain suitable molecular packing allows higher charge carrier

TABLE 3 Photovoltaic Parameters of the BHJ Solar Cell Devices Based on Polymer:PC$_{71}$BM Blends with Different Weight Ratios Processed from *o*-DCB Solvent

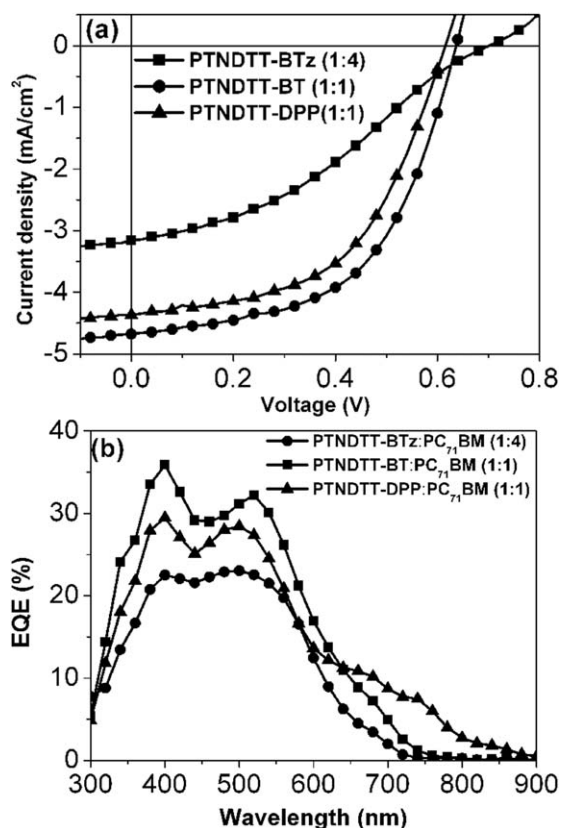| Active layer	Thickness (nm)	J_{sc} (mAcm^{-2})	V_{oc} (V)	FF	PCE (%)
PTNDTT-BTz:PC$_{71}$BM (1:1)	83	3.09	0.75	0.25	0.66
PTNDTT-BTz:PC$_{71}$BM (1:2)	80	3.07	0.71	0.31	0.67
PTNDTT-BTz:PC$_{71}$BM (1:3)	84	2.38	0.70	0.26	0.45
PTNDTT-BTz:PC$_{71}$BM (1:4)	81	3.15	0.70	0.34	0.76
PTNDTT-BT:PC$_{71}$BM (1:1)	81	4.67	0.63	0.54	1.62
PTNDTT-BT:PC$_{71}$BM (1:2)	67	3.92	0.65	0.47	1.21
PTNDTT-BT:PC$_{71}$BM (1:3)	75	0.26	0.63	0.24	0.04
PTNDTT-BT:PC$_{71}$BM (1:4)	83	0.08	0.62	0.26	0.013
PTNDTT-DPP:PC$_{71}$BM (1:1)	102	4.37	0.62	0.53	1.42
PTNDTT-DPP:PC$_{71}$BM (1:2)	87	4.03	0.61	0.58	1.42
PTNDTT-DPP:PC$_{71}$BM (1:3)	98	3.65	0.61	0.58	1.28
PTNDTT-DPP:PC$_{71}$BM (1:4)	99	3.55	0.60	0.58	1.24

FIGURE 5 (a) Current-voltage (*J-V*) and (b) external quantum efficiency (EQE) curves of the solar cells based on **PTNDTT-BTz**:$PC_{71}BM$ (1:4 w/w), **PTNDTT-BT**:$PC_{71}BM$ (1:1 w/w), and **PTNDTT-DPP**:$PC_{71}BM$ (1:1 w/w) blends in *o*-DCB.

measured under monochromatic illumination. The EQE curves of **PTNDTT-BTz**:$PC_{71}BM$ (1:4), **PTNDTT-BT**:$PC_{71}BM$ (1:1), and **PTNDTT-DPP**:$PC_{71}BM$ (1:1) devices are presented in Figure 5(b). As observed, **PTNDTT-BTz**:$PC_{71}BM$ (1:4) has a spectral response between 300 and 700 nm, with the maximum EQE being ~23% at 496 nm. In comparison, the **PTNDTT-BT**:$PC_{71}BM$ (1:1)-based device exhibits a much better spectral response in the range from 350 to 740 nm, with its maximum EQE being ~35% at 397 nm. The higher EQE of the **PTNDTT-BT**:$PC_{71}BM$ (1:1)-based device supports its higher *J*sc. However, the device based on **PTNDTT-DPP**:$PC_{71}BM$ (1:1) exhibits relatively a broad and high-coverage photoresponse, extending up to 900 nm, consistent with its absorption spectrum, but the EQE is lower at wavelengths between 370 and 540 nm with respect to **PTNDTT-BT**:$PC_{71}BM$ and higher than **PTNDTT-BTz**:$PC_{71}BM$, with the maximum being ~29% at 397 nm and 28% at 499 nm.

Morphology

Atomic force microscope images of copolymers:$PC_{71}BM$ films were taken to make an effective comparison of the surface morphology and its correlation with photovoltaic performance. Figure 6 shows the tapping mode AFM images of **PTNDTT-BTz**:$PC_{71}BM$ (1:4 w/w), **PTNDTT-BT**:$PC_{71}BM$ (1:1 w/w) and **PTNDTT-BTz**:$PC_{71}BM$ (1:1 w/w) blended films processed from *o*-dichlorobenzene. As shown in Figure 6(a), the surface morphology of **PTNDTT-BTz**:$PC_{61}BM$ blend shows a rather coarse structure with large 50–100 nm domains and a root-mean-square roughness (rms) of 8.02 nm. The larger aggregated domains reduced the polymer/acceptor interfacial area in the **PTNDTT-BTz**:$PC_{71}BM$ system. Moreover, since the typical exciton diffusion length in the disordered blend layer is ~10 nm, the larger-scale phase separation in **PTNDTT-BTz**:$PC_{71}BM$ is not favorable for efficient exciton diffusion, leading to lower J_{sc} and FF in **PTNDTT-BTz**-based devices. In contrast, **PTNDTT-BT**:$PC_{71}BM$ and **PTNDTT-DPP**:$PC_{71}BM$ blend films have smooth surfaces with root-mean square (rms) roughnesses of 2.29 and 2.36 nm, respectively, an indication of good film-forming properties and adequate miscibility with $PC_{71}BM$. The greater uniformity of the **PTNDTT-BT**:$PC_{71}BM$ and **PTNDTT-DPP**:$PC_{71}BM$ blended films with respect to the **PTNDTT-BTz**:$PC_{71}BM$ blended film leads to relatively higher J_{sc} and higher FF, and thus a better PCE in case of copolymers **PTNDTT-BTz** and **PTNDTT-DPP**. Despite showing a better photovoltaic behaviors as compared with the copolymer **PTNDTT-BTz**, the PCE values obtained so far from the copolymers **PTNDTT-BT** and **PTNDTT-DPP** however are still lower than the state-of-art photovoltaic efficiency (~8%) exhibited by the PTB series[28(a)] and the limiting factor for preventing **PTNDTT-BT** and **PTNDTT-DPP** for achieving higher PCE mainly attributed to their low J_{sc} values. Generally, the J_{sc} of PSCs depends on the absorption spectra of the polymers, their charge carrier mobility, and the morphology of the interpenetrating network of the polymer/fullerene blend active layer. Since the hole mobility of any given polymer is also known to be a function of molecular weight,[51] the low molecular weight of **PTNDTT-BT** and **PTNDTT-BTz**

mobilities in addition to higher device FFs in devices containing **PTNDTT-BT** and **PTNDTT-DPP** copolymers. However, when the V_{oc} values are compared among the copolymers, it is found that **PTNDTT-BTz**-based devices have slightly higher V_{oc} (0.70–0.75 V) values, followed in turn by the devices based on **PTNDTT-BT** (0.62–0.65 V) and **PTNDTT-DPP** (0.60–0.62 V). Because the V_{oc} value is directly proportional to the difference between the donor HOMO and the acceptor LUMO, the higher V_{oc} values of **PTNDTT-BTz**-based devices (0.70–0.75 V) could be attributed to the deep-lying HOMO level of **PTNDTT-BTz** (−5.26 eV). However, although the **PTNDTT-DPP** copolymer possesses a HOMO level 0.08 eV deeper (−5.22 eV) than that of **PTNDTT-BT** (−5.14 eV), expected to offer a higher V_{oc} in devices, the observed V_{oc} for **PTNDTT-DPP** remains almost similar or slightly lower (~0.01–0.04 eV) than that of the **PTNDTT-BT**. This unusual V_{oc} trend indicates that apart from the general frontier molecular energy levels that mostly direct the V_{oc} of the photovoltaic devices, perhaps, some other factors such as the cathode, interfacial resistances, work functions between two electrode, and nonradiative exciton recombination could play a more critical role in the V_{oc} generation of **PTNDTT-DPP**:$PC_{71}BM$-based devices.[54]

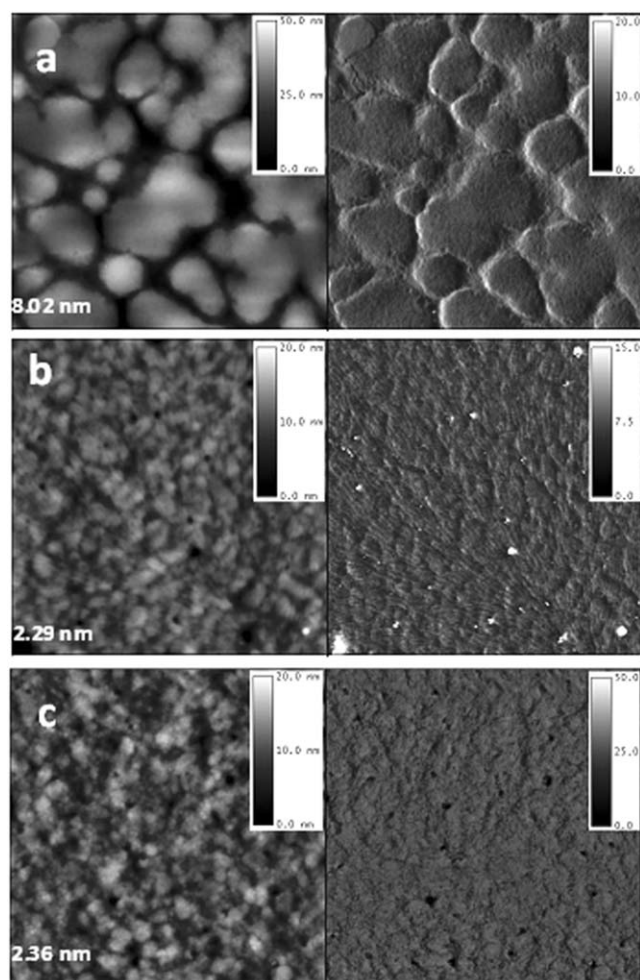To evaluate the accuracy of the *J-V* measurements, external quantum efficiencies (EQE) of the photovoltaic cells were

FIGURE 6 AFM images (2 × 2 μm²; first column: height image; second column: phase image) of films spin-coated from **PTNDTT-BTz**:PC$_{71}$BM (1:4 w/w), **PTNDTT-BT**:PC$_{71}$BM (1:1 w/w), and **PTNDTT-DPP**:PC$_{71}$BM (1:1 w/w) blends in *o*-DCB.

are indeed expected to limit the hole mobility and in turn limit the J_{sc} values of the corresponding PSCs. However, it is worth mentioning although the mobility of **PTNDTT-BTz** (7.9×10^{-5} cm² V^{-1} s^{-1}) was significantly inferior, which is consistent with its very low molecular weight, the mobility of other two copolymers, that is, **PTNDTT-BT** (2.73×10^{-3} cm² V^{-1} s^{-1}) and **PTNDTT-DPP** (2.8×10^{-4}) are within the desired range of PSC applications (i.e., $\sim 10^{-3}$ cm² V^{-1} s^{-1}). Therefore, the mobility alone should not be held responsible for low photocurrent, especially in case of copolymers **PTNDTT-BT** and **PTNDTT-DPP**. Rather, some other factors are also playing to limit the J_{sc} values in case of copolymers **PTNDTT-BT** and **PTNDTT-DPP**. To further find out the exact reason for the low J_{sc}, we have taken the photoluminescence (PL) spectra of pristine copolymers and their composites with PC$_{71}$BM. The PL spectra of **PTNDTT-BTz**/PC$_{71}$BM, **PTNDTT-BT**/PC$_{71}$BM and **PTNDTT-DPP**/PC$_{71}$BM are shown in Supporting Information Figure S9. As shown, the emission spectra of all three copolymers get completely quenched when they are blended with PC$_{71}$BM. Therefore, the electron

transfer from the photoexcited polymers to PC$_{71}$BM can effectively takes place. Thus, the major factor for the low J_{sc} must be due to not obtaining an ideal morphology of the active layers. We believe that the J_{sc} value could be improved further by using different solvents, adding various additives. Hence, some optimized work for the devices need to be carried out to improve it further, which is currently being considered in our group.

CONCLUSIONS

In summary, a series of naphtho[1,2-*b*:5,6-*b'*]dithiophene-containing D-A conjugated polymers, **PTNDTT-BTz**, **PTNDTT-BT**, and **PTNDTT-DPP** were designed and synthesized by Stille polymerization incorporating thiophene-bridged naphtho[1,2-*b*:5,6-*b'*]dithiophene as a donor unit and **BTz**, **BT**, and pyrrolo[3,4-c]pyrrole-1,4(2H,5H)-dione (**DPP**) as acceptor units. The copolymers possessed good solubility, excellent processability, and high thermal stability, properties considered requisite for efficient photovoltaic applications. The incorporation of different electron-deficient units help to modulate the band gap of these naphtho[1,2-*b*:5,6-*b'*]dithiophene-based copolymers from 1.58 to 1.9 eV. The HOMO and LUMO energy levels of these copolymers were also found to be effectively tuned from −5.14 to −5.26 eV and −3.13 to −3.26 eV, respectively. The preliminary PSC based on the blend of **PTNDTT-BTz** and PC$_{71}$BM (1:4 w/w) exhibited a PCE of 0.76% with a Jsc of 3.15 mA cm^{-2}, a Voc of 0.70 V, and a FF of 0.34. In comparison, the cells processed from **PTNDTT-BT**:PC$_{71}$BM (1:1, w/w) or **PTNDTT-DPP**:PC$_{71}$BM (1:1, w/w) delivered improved performance with PCEs of 1.62 and 1.42%, respectively. The higher PCE for **PTNDTT-BT** and **PTNDTT-DPP** compared with **PTNDTT-BTz** was attributed to a combination of higher molecular masses, broader absorption, higher mobility, and more suitable phase separation, thus enabling improved Jsc and FF. The results of preliminary photovoltaic studies suggest that these new copolymers derived from naphtho[1,2-*b*:5,6-*b'*]dithiophene donor units are promising photovoltaic donor materials. Detailed optimizations of the corresponding PSCs are currently under progress in our laboratory, which could support further the potential of these new copolymers for delivering high efficiency.

REFERENCES AND NOTES

1 G. Yu, J. Gao, J. C. Hummelen, F. Wudl, A. Heeger, *J. Science* **1995**, *270*, 1789–1791.

2 C. J. Brabec, N. S. Sariciftci, J. C. Hummelen, *Adv. Funct Mater.* **2001**, *11*, 15–26.

3 K. M. Coakley, M. D. McGehee, *Chem. Mater.* **2004**, *16*, 4533–4542.

4 J. Y. Kim, K. Lee, N. E. Coates, D. Moses, T. Q. Nguyen, M. Dante, A. Heeger, *J. Science* **2007**, *317*, 222–225.

5 (a) S. Gunes, H. S. Neugebauer, N. S. Sariciftci, *Chem. Rev.* **2007**, *107*, 1324–1338; (b) J. Peet, J. Y. Kim, N. E. Coates, W. L. Ma, D. Moses, A. J. Heeger, G. C. Bazan, *Nat. Mater.* **2007**, *6*, 497–500.

6 (a) B. C. Thompson, J. M. J. Frechet, *Angew. Chem. Int. Ed.* **2008**, *47*, 58–77; (b) Y. Li, Y. Zou, *Adv. Mater.* **2008**, *20*, 2952–2958.

7 (a) G. Dennler, M. C. Scharber, C. J. Brabec, *Adv. Mater.* **2009**, *21*, 1323–1338; (b) Y. J. Cheng, S. H. Yang, C. S. Hsu, *Chem. Rev.* **2009**, *109*, 5868–5923; (c) J. Peet, M. L. Senatore, A. J. Heeger, G. C. Bazan, *Adv. Mater.* **2009**, *21*, 1521–1527; (d) H.-Y. Chen, J. Hou, S. Zhang, Y. Liang, G. Yang, Y. Yang, L. Yu, Y. Wu, G. Li, *Nat. Photon.* **2009**, *3*, 649–653.

8 L. Huo, J. Hou, S. Zhang, H.-Y. Chen, Y. Yang, *Angew. Chem.* **2010**, *122*, 1542–1545.

9 G. Li, R. Zhu, Y. Yang, *Nat. Photon.* **2012**, *6*, 153–161.

10 Z. He, C. Zhong, X. Huang, W. Wong, H. Wu, L. Chen, S. Su, Y Cao, *Adv. Mater.* **2011**, *23*, 4636–4643.

11 L. T. Dou, J. B. You, J. Yang, C.-C. Chen, Y. J. He, S. Murase, T. Moriarty, K. Emery, G. Li, Y. Yang, *Nat. Photon.* **2012**, *6*, 180–185.

12 C. E. Small, S. Chen, J. Subbiah, C. M. Amb, S.-W. Tsang, T.-H. Lai, J. R. Reynolds, F. So, *Nat. Photon.* **2012**, *6*, 115–120.

13 X. H. Li, W. C. H. Choy, L. J. Huo, F. X. Xie, W. E. I. Sha, B. F. Ding, X. Guo, Y. F. Li, J. H. Hou, J. B. You, Y. Yang, *Adv. Mater.* **2012**, *24*, 3046–3052.

14 S. Chen, C. E. Small, C. M. Amb, J. Subbiah, T. H. Lai, S. W. Tsang, J. R. Manders, J. R. Reynolds, F. So, *Adv. Energy Mater.* **2012**, *2*, 1333–1337.

15 H.-C. Chen, Y.-H. Chen, C.-C. Liu, Y.-C. Chien, S.-W. Chou, P.-T. Chou, *Chem. Mater.* **2012**, *24*, 4766–4772.

16 S. H. Park, A. Roy, S. Beaupre, S. Cho, N. Coates, J. S. Moon, D. Moses, M. Leclerc, K. Lee, A. J. Heeger, *Nat. Photon.* **2009**, *3*, 297–302.

17 L. Huo, S. Zhang, X. Guo, F. Xu, Y. Li, J. Hou, *Angew. Chem. Int. Ed.* **2011**, *50*, 9697–9702.

18 Y. Liang, Z. Xu, J. Xia, S.-T. Tsai, Y. Wu, G. Li, C. Ray, L. Yu, *Adv. Mater.* **2010**, *22*, E135–E138.

19 C. M. Amb, S. Chen, K. R. Graham, J. Subbiah, C. E. Small, F. So, J. R. J. Reynolds, *Am. Chem. Soc.* **2011**, *133*, 10062–10065.

20 T.-Y. Chu, J. Lu, S. Beaupré, Y. Zhang, J.-R. Pouliot, S. Wakim, J. Zhou, M. Leclerc, Z. Li, J. Ding, Y. Tao, *J. Am. Chem. Soc.* **2011**, *13*, 4250–4252.

21 M.-S. Su, C.-Y. Kuo, M.-C. Yuan, U. S. Jeng, C.-J. Su, K.-H. Wei, *Adv. Mater.* **2011**, *23*, 3315–3319.

22 H. Zhou, L. Yang, A. C. Stuart, S. C. Price, S. Liu, W. You, *Angew. Chem. Int. Ed.* **2011**, *50*, 2995–2998.

23 Y. Sun, C. J. Takacs, S. R. Cowan, J. H. Seo, X. Gong, A. Roy, A. J. Heeger, *Adv. Mater.* **2011**, *23*, 2226–2230.

24 S. C. Price, A. C. Stuart, L. Yang, H. Zhou, W. You, *J. Am. Chem. Soc.* **2011**, *133*, 4625–4631.

25 J. H. Hou, H. Y. Chen, S. Q. Zhang, G. Li, Y. Yang, *J. Am. Chem. Soc.* **2008**, *130*, 16144–16145.

26 (a) M. Zhang, X. Guo, X. Wang, H. Wang, Y. Li, *Chem. Mater.* **2011**, *23*, 4264–4270; (b) J. C. Bijleveld, A. P. Zoombelt, S. G. J. Mathijssen, M. M. Wienk, M. Turbiez, D. M. de Leeuw, R. A. J. Janssen, *J. Am. Chem. Soc.* **2009**, *131*, 16616–16617.

27 (a) N. Blouin, A. Michaud, M. A. Leclerc, *Adv. Mater.* **2007**, *19*, 2295–2300; (b) R. Li Qin, W. Li, C. Du, C. Veit, H. F. Schleiermacher, M. Andersson, Z. Bo, Z. Liu, O. Inganäs, U. Wuerfel, F. Zhang, *J. Am. Chem. Soc.* **2009**, *131*, 14612–14613; (c) L. J. Zhang, C. He, J. W. Chen, P. Yuan, L. A. Huang, C. Zhang, W. Z. Cai, Z. T. Liu, Y. Cao, *Macromolecules* **2010**, *43*, 9771–9778.

28 (a) Y. Y. Liang, L. P. Yu, *Acc. Chem. Res.* **2010**, *43*, 1227–1236; (b) H. J. Son, W. Wang, T. Xu, Y. Liang, Y. Wu, G. Li, L. Yu, *J. Am. Chem. Soc.* **2011**, *133*, 1885–1894; (c) Y. Huang, X. Guo, F. Liu, L. Huo, Y. Chen, T. P. Russell, C. C. Han, Y. Li, J. Hou, *Adv. Mater.* **2012**, *24*, 3383–3389.

29 (a) Z. Zhu, D. Waller, R. Gaudiana, M. Morana, D. Muhlbacher, M. Scharber, C. Brabec, *Macromolecules* **2007**, *40*, 1981–1986; (b) J. C. Bijleveld, M. Shahid, J. Gilot, M. M. Wienk, R. A. J. Janssen, *Adv. Funct. Mater.* **2009**, *19*, 3262–3270; (c) Z. Li, J. Ding, N. Song, J. Lu, Y. Tao, *J. Am. Chem. Soc.* **2010**, *132*, 13160–13161.

30 (a) J. Hou, H. Chen, S. Zhang, G. Li, Y. Yang, *J. Am. Chem. Soc.* **2008**, *130*, 16144–16145; (b) M. Zhang, H. Fan, X. Guo, Y. He, Z. Zhang, J. Min, J. Zhang, X. Zhan, Y. Li, *Macromolecules* **2010**, *43*, 5706–5712; (c) M. Zhang, X. Guo, Y. Li, *Adv. Energy Mater.* **2011**, *1*, 557–560; (d) Z. Zhang, J. Min, S. Zhang, J. Zhang, Y. Li, *Chem. Commun.* **2011**, *47*, 9474–9476.

31 (a) Y. Chen, C. Yu, Y. Fan, L. Hung, C. Chen, C. Ting, *Chem. Commun.* **2010**, *46*, 6503–6505; (b) Y. Zhang, J. Zou, H. Yip, K. Chen, J. Davies, Y. Sun, A. Jen, *Macromolecules* **2011**, *44*, 4752–4758; (c) M. Zhang, X. Guo, X. Wang, H. Wang, Y. Li, *Chem. Mater.* **2011**, *23*, 4264–4270.

32 (a) L. Huo, J. Hou, S. Zhang, H.-Y. Chen, Y. Yang, *Angew. Chem., Int. Ed.* **2010**, *49*, 1500–1503; (b) J.-Y. Wang, S. K. Hau, H.-L. Yip, J. A. Davies, K.-S. Chen, Y. Zhang, Y. Sun, A. K. Y. Jen, *Chem. Mater.* **2011**, *23*, 765–767; (c) N. Allard, R. B. Aich, D. Gendron, P.-L. T. Boudreault, C. Tessier, S. Alem, S.-C. Tse, Y. Tao, M. Leclerc, *Macromolecules* **2010**, *43*, 2328–2333.

33 (a) K.-C. Li, J.-H. Huang, Y.-C. Hsu, P.-J. Huang, C.-W. Chu, J.-T. Lin, K.-C. Ho, K.-H. Wei, H.-C Lin, *Macromolecules* **2009**, *42*, 3681–3693; (b) M. Zhang, H. Fan, X. Guo, Y. He, Z.-G. Zhang, J. Min, J. Zhang, G. Zhao, X. Zhan, Y. Li, *Macromolecules* **2010**, *43*, 8714–8717; (c) Q. Shi, H. Fan, Y. Liu, J. Chen, L. Ma, W. Hu, Z. Shuai, Y. Li, X. Zhan, *Macromolecules* **2011**, *44*, 4230–4240.

34 (a) M. Zhang, X. Guo, Y. Li, *Adv. Energy Mater.* **2011**, *1*, 557–560; (b) S. Subramaniyan, H. Xin, F. S. Kim, S. A. Jenekhe, *Macromolecules* **2011**, *44*, 6245–6248; (c) S. K. Lee, J. M. Cho, Y. Goo, W. S. Shin, J.-C. Lee, W.-H. Lee, I.-N. Kang, H.-K. Shim, S.-J. Moon, *Chem. Commun.* **2011**, *47*, 1791–1793.

35 (a) Z. He, C. Zhang, X. Xu, L. Zhang, L. Huang, J. Chen, H. Wu, Y. Cao, *Adv. Mater.* **2011**, *23*, 3086–3089; (b) E. Wang, L. Hou, Z. Wang, S. Hellström, F. Zhang, O. Inganäs, M. R. Andersson, *Adv. Mater.* **2010**, *22*, 5240–5244; (c) J. Zhang, W. Z. Cai, F. Huang, E. G. Wang, C. M. Zhong, S. J. Liu, M. Wang, C. H. Duan, T. B. Yang, Y. Cao, *Macromolecules* **2011**, *44*, 894–901.

36 (a) Y. Zhang, J. Y. Zou, H. L. Yip, Y. Sun, J. A. Davies, K. S. Chen, O. Acton, A. K. Y. Jen, *J. Mater. Chem.* **2011**, *21*, 3895–3902; (b) Z. Li, S. W. Tsang, X. M. Du, L. Scoles, G. Robertson, Y. G. Zhang, F. Toll, Y. Tao, J. P. Lu, J. F. Ding, *Adv. Funct. Mater.* **2011**, *21*, 3331–3336.

37 (a) J. C. Bijleveld, A. P. Zoombelt, S. G. J. Mathijssen, M. M. Wienk, M. Turbiez, D. M. de Leeuw, R. A. J. Janssen, *J. Am. Chem. Soc.* **2009**, *131*, 16616–16617; (b) N. Allard, R. B. Aïch, D. Gendron, P.-L. T. Boudreault, C. Tessier, S. Alem, S.-C. Tse, Y. Tao, M Leclerc, *Macromolecules* **2010**, *43*, 2328–2333; (c) J. C. Bijleveld, V. S. Gevaerts, D. Di Nuzzo, M. Turbiez, S. G. J.

Mathijssen, D. M. de Leeuw, M. M. Wienk, R. A. J. Janssen, *Adv. Mater.* **2010**, *22*, E242–E246.

38 (a) S. Loser, C. J. Bruns, H. Miyauchi, R. P. Ortiz, A. Facchetti, S. I. Stupp, T. J. Marks, *J. Am. Chem. Soc.* **2011**, *133*, 8142–8145; (b) S. Loser, H. Miyauchi, J. W. Hennek, J. Smith, C. Huang, A Facchetti. T. J. Marks, *Chem. Commun.* **2012**, *48*, 8511–8513.

39 S. R. Sanjaykumar, S. Badgujar, C. E. Song, W. S. Shin, S.-J. Moon, I.-N. Kang, J. Lee, S. Cho, S. K. Lee, J.-C. Lee, *Macromolecules* **2012**, *45*, 6938–6945.

40 B. Rungtaweevoranit, A. Butsuri, K. Wongma, K. Sadorn, K. Neranon, C. Nerungsi, T. Thongpanchang, *Tetrahedron Lett.* **2012**, *53*, 1816–1818.

41 (a) H. Zhou, Y. Liqiang, S. Liu, W. You, *Macromolecules* **2010**, *43*, 10390–10396; (b) L. Yang, H. Zhou, W. You, *J. Phys. Chem. C* **2010**, *114*, 16793–16800; (c) H. Zhou, L. Yang, S. Stoneking, W. You, *ACS Appl. Mater. Interfaces* **2010**, *2*, 1377–1383; (d) N. Kleinhenz, L. Yang, H. Zhou, S. C. Price, W. You, *Macromolecules*, **2011**, *44*, 872–877.

42 I. Osaka, S. Shinamura, T. Abe, K Takimiya, J. *Mater. Chem C.*, **2013**, *1*, 1297–1304.

43 I. Osaka, T. Abe, S. Shinamura, E. Miyazaki, K. Takimiya, *J. Am. Chem. Soc.* **2010**, *132*, 5000–5001.

44 (a) P. Dutta, W. Yang, S. H. Eom, W.-H. Lee, I.-N. Kang, S.-H. Lee, *Chem. Commun.* **2012**, *48*, 573–575; (b) P. Dutta, W. Yang, W.-H. Lee, I. N. Kang, S.-H. Lee, *J. Mater. Chem.* **2012**, *22*, 10840–10851.

45 (a) P. Dutta, H. Park, W. H. Lee, K. Kim, I. N. Kang, S.-H. Lee, *Polym. Chem.* **2012**, *3*, 601–604; (b) A. V. Patil, W.-H. Lee, K. Kim, H. Park, I.-N. Kang, S.-H. Lee, *Polym. Chem.* **2011**, *2*, 2907–2916.

46 I. Osaka, T. Abe, M. Shimawaki, T. Koganezawa, K. Takimiya, *ACS Macro Lett.* **2012**, *1*, 437–440.

47 H. Bronstein, Z. Chen, R. S. Ashraf, W. Zhang, J. Du, J. R. Durrant, P. S. Tuladhar, K. Song, S. E. Watkins, Y. Geerts, M. M. Wienk, R. A. J. Janssen, T. Anthopoulos, H. Sirringhaus, M. Heeney, I. McCulloch, *J. Am. Chem. Soc.* **2011**, *133*, 3272–3275.

48 G. Li, V. Shrotriya, Y. Yao, J. Huang, Y. Yang, *J. Mater. Chem.* **2007**, *17*, 3126–3140.

49 D. H. Kim, B.-L. Lee, H. Moon, H. M. Kang, E. J. Jeong, J. Park, K.-M. Han, S. Lee, B. W. Yoo, B. W. Koo, J. Y. Kim, W. H. Lee, K. Cho, H. A. Becerril, Z. Bao, *J. Am. Chem. Soc.* **2009**, *131*, 6124–6132.

50 (a) P.-T. Wu, F. S. Kim, R. D. Champion, S. A. Jenekhe, *Macromolecules* **2008**, *41*, 7021–7028; (b) B. Pal, W.-C. Yen, J.-S. Yang, C.-Y. Chao, Y.-C. Hung, S.-T. Lin, C.-H. Chuang, C.-W. Chen, W.-F. Su, *Macromolecules* **2008**, *41*, 6664–6671; (c) M.-C. Yuan, M.-Y. Chiu, C.-M. Chiang, K.-H. Wei, *Macromolecules* **2010**, *43*, 6270–6277.

51 (a) R. J. Kline, M. D. McGehee, E. N. Kadnikova, J. Liu, J. M. J. Frechet, M. F. Toney, *Macromolecules* **2005**, *38*, 3312–3319; (b) P. T. Wu, T. Bull, F. S. Kim, C. K. Luscombe, S. A. Jenekhe, *Macromolecules* **2009**, *42*, 671–681.

52 (a) Y. Deng, Y. Chen, X. Zhang, H. Tian, C. Bao, D. Yan, Y. Geng, F. Wang, *Macromolecules* **2012**, *45*, 8621–8627; (b) Y. Han, L. Chen, Y. Chen, *J. Polym. Sci. Part A: Polym. Chem.* **2013**, *51*, 258–266; (c) J. Huang, C. Zhan, X. Zhang, Y. Zhao, Z. Lu, H. Jia, B. Jiang, J. Ye, S. Zhang, A. Tang, Y. Liu, Q. Pei, J. Yao, *ACS Appl. Mater. Interfaces*, **2013**, *5*, 2033–2039.

53 (a) G. Lu, H. Usta, C. Risko, L. Wang, A. Facchetti, M. A. Ratner, T. J. Marks, *J. Am. Chem. Soc.* **2008**, *130*, 7670–7685; (b) S. Subramaniyan, H. Xin, F. S. Kim, S. A. Jenekhe, *Macromolecules* **2011**, *44*, 6245–6248.

54 (a) A. Gadisa, M. Svensson, M. R. Andersson, O. Inganas, *Appl. Phys. Lett.* **2004**, *84*, 1609–1611; (b) B. P. Rand, D. P. Burk, S. R. Forrest, *Phys. Rev. B* **2007**, *75*, 115327; (c) D. Veldman, S. C. J. Meskers, R. A. J. Janssen, *Adv. Funct. Mater.* **2009**, *19*, 1939–1948; (d) J. Luo, H. B. Wu, C. He, A. Y. Li, W. Yang, Y. Cao, *Appl. Phys. Lett.* **2009**, *95*, 043301–043303; (e) K. Vandewal, K. Tvingstedt, A. Gadisa, O. Inganas, J. V. Manca, *Nature Mater.* **2009**, *8*, 904–909; (f) C. He, C. M. Zhong, H. B. Wu, R. Q. Yang, W. Yang, F. Huang, G. C. Bazan, Y. Cao, *J. Mater. Chem.* **2010**, *20*, 2617–2622.